UDC 303.732.4:629.1 DOI: 10.18698/0236-3933-2020-4-22-41

SYNTHESIS OF ACTIVE DISTURBANCE REJECTION CONTROL

M. Alhelou muhammed.alhelou@gmail.com
A.I. Gavrilov alexgavrilov@bmstu.ru

Bauman Moscow State Technical University, Moscow, Russian Federation

Abstract

Synthesis of Active Disturbance Rejection Control (ADRC) has been discussed in this work. Two main approaches have been presented for the second-order ADRC: Linear ADRC and nonlinear ADRC. A design procedure for the three main components of ADRC: controller, estimator, and disturbance rejection scheme has been presented in each approach. Parameters of the linear approach are tuned using the desired closed loop system bandwidth. Parameters of the nonlinear approach are selected by categorizing them first into usual parameters and key parameters. After that, the key parameters are optimized using Genetic Algorithm (GA). The two approaches have been tested on a quarter-car system that deals with the passenger comfort problem. Simulation results show a good performance and a good compensation for external disturbances and dynamic uncertainties

Keywords

General disturbances, estimator, tracking differential, nonlinear state error feedback

Received 18.12.2019
Accepted 12.05.2020

Introduction. Active Disturbance Rejection Control (ADRC) is a control method or a strategy intended to transcend complexity of the traditional control methods such as proportional-integral-derivative (PID). ADRC is inherited from PID and can be considered as a robust control method. It represents all unknown dynamics which are not included in the mathematical model of the controlled system. Moreover; it compensates for the modeling uncertainties and external perturbations in real time.

ADRC has dynamic methodology and unnecessary knowledge of a plant precise model [1–3]. Therefore, various applications use ADRC as a replacement for the classic controllers.

ADRC is a process that aims to reject the unknown internal dynamics of a plant and the external disturbances in real time. It depends on forcing the controlled plant to behave as an n-order integrator system which is easily

controlled by a PD controller, even if the plant is nonlinear and time-variant. For doing so, an estimation for the nonlinear and time-variant internal dynamics has been performed. Moreover; a prediction of the external disturbances is conducted to reject these disturbances from the whole system. The unknown dynamics and the external disturbances could be combined together in "General Disturbances" then estimated and rejected.

ADRC has been widely used since its beginning in the nineties of the last century. It inherits from PID little overshoot, high convergence speed, high accuracy, strong anti-interference ability and other characteristics [4]. It depends on expanding the system model to include everything the user does not include in the mathematical description. Zhu E., et al. in [5] proposed an ADRC control based method for an airship to track a trajectory. Internal dynamic uncertainties and external disturbances are estimated by an Extended State Observer (ESO). ADRC is used to realize the decoupling control for multivariable systems. Simulation results show steady and rapid responses. Results have been compared with a sliding mode control (SMC) results and showed more steady performance.

Li X., et al. in [6] used ADRC in order to improve the control of permanent magnet brushless motor. The authors presented the second order form of ADRC. Discrete equations of the tracking differentiator (TD), the extended state observer (ESO), and the nonlinear-state error feedback (NLSEF) were shown. Simulation results of the motor controlled system, based on ADRC, were displayed. The anti-disturbance capability of the system was presented by adding a square wave at a specific time point and system reaction was observed. Simulation results showed that TD and ESO can ensure the ability of tracking the input and output.

Gao Z., et al. in the United States patent [7] presented multiple designs and methods to control a system using ADRC. The authors presented a precise design for ADRC to control a second order system. ESO and TD parameters were chosen as functions of the system bandwidth. A discrete implementation of ADRC was presented and gain matrices of its components were shown. The authors claimed that a generalized form of ADRC to control an n-th order system can be presented in the same manner. A new design called Predictive Active Disturbance Rejection Controller was proposed. The basic design principles for this controller were explained and a compatible Reduced order ESO (RESO) was used.

Peng C., et al. in [8] proposed an ADRC trajectory tracking control based on Particle Swarm Optimization (PSO) for a quad-rotor (QR) system. PSO is used to adjust and optimize parameters of ADRC so as to enhance the system design efficiency. A dynamic model for QR was presented and the three impediments

of the ADRC controller: TD, ESO and NLSEF were proposed. The TD unit in the altitude z channel was designed based on fast discrete tracking differentiator method as in [9]. New equation based forms for ESO and NLSEF were presented. The quad-rotor closed loop system was divided into four independent channels by ADRC. Controller optimization using PSO was applied to the four channels respectively.

Wang Ch., et al. in [10] addressed the problem of steering Underactuated Surface Vessels (USVs) along given paths. ADRC technique was proposed to eliminate dynamic uncertainty and ocean disturbances induced by unknown wind, waves, and ocean currents. Second-order ADRC was used to control the equivalent rudder angle by the propeller rate. Blocks based MATLAB Simulation was used to simulate the proposed USV system, ADRC parameter optimization using Chaos PSO (CPSO) for clamping force control system in order to achieve higher control precision, designed equations for TD, ESO, and NLSEF, CPSO algorithm to minimize a fitness function J which is a function of time, error, and control signal.

Simulation results showed better performance when using ADRC with PSO optimization algorithm in comparison with using ADRC alone.

ADRC Approaches. In this section, two approaches of second-order ADRC controller are presented.

Linear ADRC. The linear ADRC is described based on the American patent [7]. Fig. 1 shows the contents of a linear ADRC structure.

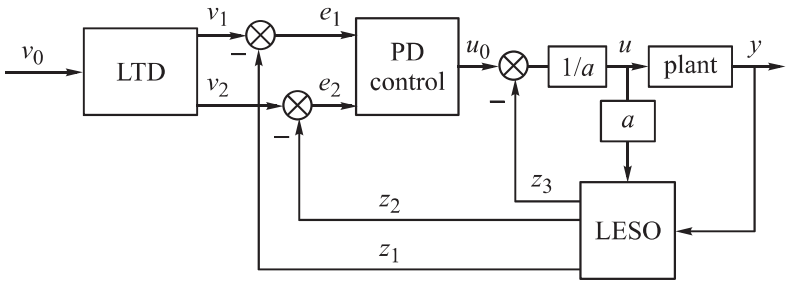

Fig. 1. Linear ADRC structure

This structure consists of controller, linear estimator (Linear Extended State Observer (LESO)), linear tracking differentiator (LTD) and a disturbance rejection scheme.

Linear Tracking Differentiator (LTD). Using LTD, the reference signal is smoothed and output signals are generated to track the reference signal and its difference. The designed algorithm is as follows:

$$\begin{aligned} \dot{v}_1 &= v_2; \\ \dot{v}_2 &= -k_1(v_1 - v_0) - k_2 v_2, \end{aligned} \tag{1}$$

where v_0 is the reference signal, v_1 is the tracking signal of the system and v_2 is the differential signal of the system. Here k_1, k_2 are adjustable parameters of LTD. When $k_1 = r^2;\ k_2 = 2r;\ r > 0,$ the transition process is not overshoot, and transition time is about $T_0 = 7/r,$ r is speed factor.

Linear Extended State Observer. The idea behind ESO is capturing information about the generalized disturbances (uncertainties and external disturbances $\hat{f}$) and the internal dynamics of the system ($\hat{y}$, $\hat{\dot{y}}$).

System dynamics can be expressed in the following general form:

$$\ddot{y} = g(t, y, \dot{y}) + au + w, \tag{2}$$

where y is the output signal, u is the control input, $g(.)$ is the dynamic of the plant (including the unknown dynamics), w is the external disturbance, and a is the system coefficient. All parts of this dynamics $(g(.), a, w)$ are usually not precisely known. By combining the external and the internal disturbances in one function $f(.)$ the dynamic can be written as:

$$\ddot{y} = f(t, y, \dot{y}, w) + au. \tag{3}$$

Equation (3) can be written in state space in the form:

$$\begin{aligned} \dot{x}_1 &= x_2; \\ \dot{x}_2 &= f + au; \\ y &= x_1. \end{aligned} \tag{4}$$

The total disturbance is augmented with the states in the following way:

$$\begin{aligned} \dot{x}_1 &= x_2; \\ \dot{x}_2 &= x_3 + au; \\ \dot{x}_3 &= \dot{f}(t, x_1, x_2, w); \\ y &= x_1. \end{aligned} \tag{5}$$

This can be expressed in the vector-matrix form as:

$$\begin{aligned} \dot{x} &= A_x x + B_x u + E_x \dot{f}; \\ y &= C_x x, \end{aligned} \tag{6}$$

where

$$A_x = \begin{bmatrix} 0 & 1 & 0 \\ 0 & 0 & 1 \\ 0 & 0 & 0 \end{bmatrix}, \quad B_x = \begin{bmatrix} 0 \\ a \\ 0 \end{bmatrix}, \quad C_x = \begin{bmatrix} 1 & 0 & 0 \end{bmatrix}, \quad E_x = \begin{bmatrix} 0 \\ 0 \\ 1 \end{bmatrix}. \tag{7}$$

A linear ESO (LESO) can be used here to estimate the states x_1, x_2, x_3. This way, LESO can be designed to be:

$$\begin{aligned} \dot{z}_1 &= z_2 + \alpha_1 \hat{e}; \\ \dot{z}_2 &= z_3 + \hat{a}u + \alpha_2 \hat{e}; \\ \dot{z}_3 &= + \alpha_3 \hat{e}, \end{aligned} \tag{8}$$

where z_1, z_2 and z_3 are the approximated values of states x_1, x_2 and x_3 respectively, α_1, α_2 and α_3 are the observer gains, and $\hat{e} = y - z_1$ is the estimated error of x_1, $\hat{a}$ is an estimated value for a in equation (2) and it can be chosen empirically in this structure.

The estimated variables ($z_1 = \hat{y}$, $z_2 = \hat{\dot{y}}$, $z_3 = \hat{f}$) besides the approximated value $\hat{a}$ are then used to eliminate the disturbance and control the system as shown in Fig. 1.

Disturbance rejection scheme. The disturbance rejection scheme can be defined as:

$$u = \frac{u_0 - z_3}{\hat{a}} = \frac{u_0 - \hat{f}}{\hat{a}}, \tag{9}$$

where u is the rejection scheme output and u_0 is the control part output. By replacing u by its estimated value in equation (2):

$$\ddot{y} = f(.) + a\left(\frac{u_0 - \hat{f}}{\hat{a}}\right). \tag{10}$$

If the estimator is good enough to consider that $\hat{a} \approx a$ and $\hat{f} \approx f$, then the plant can be written as a second order integrator:

$$\ddot{y} \approx u_0. \tag{11}$$

Feedback controller. If a proportional-derivative (PD) controller is used as a feedback controller, the control signal u_0 can be written in the form

$$u_0(t) = K_p(v_0 - \hat{y}) + K_d\hat{\dot{y}}, \tag{12}$$

where v_0 is the reference input. PD gains can be chosen as

$$K_p = w_{CL}^2, \quad K_d = -2\xi w_{CL}, \tag{13}$$

where w_{CL} is the desired closed loop pole and ξ is the desired damping coefficient of the closed loop.

For observing poles, w_{ESO} should be placed n times to the left of the closed loop pole to ensure that the dynamics of the observer are faster enough than the dynamics of the controlled plant, where $n \in [3, 10]$, i.e.,

$$w_{\text{ESO}} = nw_{CL}. \tag{14}$$

For simplicity, all the observer poles are placed in one location. That means, the characteristic equation of the observer is:

$$D(\lambda) = (\lambda + w_{\text{ESO}})^3 = \lambda^3 + 3w_{\text{ESO}}\lambda^2 + 3w_{\text{ESO}}^2\lambda + w_{\text{ESO}}^3, \tag{15}$$

where λ represents Eigen values and $\alpha_1, \alpha_2, \alpha_3$ are calculated by solving the equation

$$D(\lambda) = |sI - A_x + LC_x|, \tag{16}$$

where s is Laplace frequency parameter and

$$I = \begin{bmatrix} 1 & 0 & 0 \\ 0 & 1 & 0 \\ 0 & 0 & 1 \end{bmatrix}, \quad L = \begin{bmatrix} \alpha_1 \\ \alpha_2 \\ \alpha_3 \end{bmatrix}. \tag{17}$$

As a result, the estimator gains can be chosen as

$$\alpha_1 = 3w_{\text{ESO}}, \quad \alpha_2 = 3w_{\text{ESO}}^2, \quad \alpha_3 = w_{\text{ESO}}^3. \tag{18}$$

Nonlinear ADRC. Fig. 2 shows a typical second order nonlinear ADRC scheme.

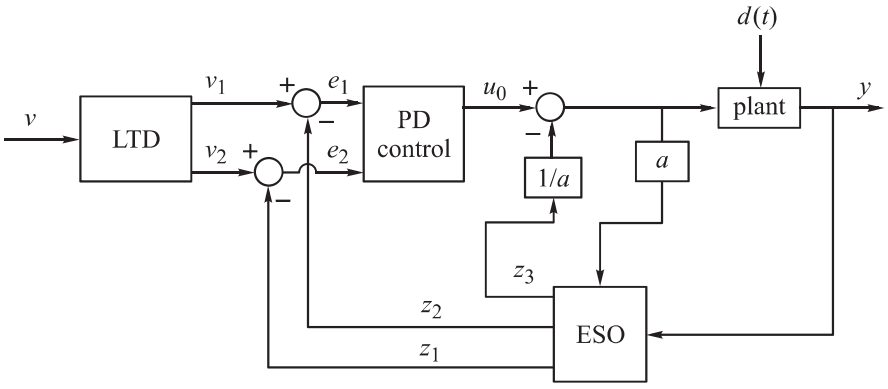

Fig. 2. Nonlinear ADRC structure

Similar to linear structure, ADRC consists of two main loops: the feedback loop and the estimation loop. It has three main components: the Tracking Differential (TD), ESO and a NLSEF.

Tracking Differential. TD is used for arranging the transient process, which can be expressed as:

$$\begin{aligned} &\dot{v}_1 = v_2; \\ &\dot{v}_2 = f_{\text{TD}}(v_1 - v_0, v_2, r) = -r\,\text{sign}\left(v_1 - v_0 + \frac{v_2|v_2|}{2r}\right), \end{aligned} \tag{19}$$

where v_0 is the input signal, v_1 is the tracking signal of v_0, v_2 is the differential signal of v_1, r is the parameter which determines the tracking speed.

The nonlinear function f_{TD} is proposed in [11] to provide the fastest tracking of the reference signal and its derivative subject to the acceleration limit of r.

The parameter r is an application dependent and it is set accordingly to speed up or slow down the transient profile.

Extended State Observer. As for the linear structure, ESO is employed to monitor the output and predict the real-time state of the plant. It can be expressed as follows [12]:

$$\begin{aligned} \hat{e} &= z_1 - y; \\ \dot{z}_1 &= z_2 + \alpha_1 \hat{e}; \\ \dot{z}_2 &= z_3 + \alpha_2 \left|\hat{e}\right|^{1/2} \operatorname{sign} \hat{e} + \hat{a}u; \\ \dot{z}_3 &= \alpha_3 \left|\hat{e}\right|^{1/4} \operatorname{sign} \hat{e}, \end{aligned} \tag{20}$$

where y is the system output, z_1 is the tracking signal of y, $\hat{e}$ is the estimated error, z_2 is the differential signal of z_1, z_3 is the tracking signal of general disturbances, α_1, α_2 and α_3 are estimator gains, u is the control input, and $\hat{a}$ is the system coefficient.

Nonlinear State Error Feedback and disturbance rejection process. NLSEF is a nonlinear control strategy which can enhance the precision for control system. It can be expressed as follows:

$$\begin{aligned} \hat{e}_1 &= v_1 - z_1; \\ \hat{e}_2 &= v_2 - z_2; \\ u_0 &= \beta_1 f_{nl}(\hat{e}_1, \gamma_1, \eta) + \beta_2 f_{nl}(\hat{e}_2, \gamma_2, \eta); \\ u &= u_0 - \frac{z_3}{a}, \end{aligned} \tag{21}$$

where $\hat{e}_1$ is the estimated system error, $\hat{e}_2$ is the estimated differential of system error, β_1 and β_2 are gain coefficients, and z_3 / a is the total disturbance compensation of the system; f_{nl} should achieve good control effect and high frequency tremor, and it can be chosen as [12]:

$$f_{nl}(e, \gamma, \eta) = \begin{cases} \dfrac{e}{\eta^{\gamma-1}}, & |e| \le \eta; \\ |e|^{\gamma} \operatorname{sign} e, & |e| > \eta. \end{cases} \tag{22}$$

Discrete implementation of ADRC. ADRC is implemented in discrete time. Discretization can be done using Euler or zero order hold (ZOH).

Discretization of linear ADRC. In discrete implementation of the linear ADRC, the ESO pole is determined in Z domain using the following equation [4]:

$$D_z(z) = |zI - \Phi + L_p C_x| = (z - \alpha)^3, \quad \alpha = e^{-w_{\text{ESO}}h}, \tag{23}$$

where h is sampling time, L_p is the observer gain matrix, C_x is the plant observation matrix, and Φ is the plant discrete state matrix.

In [7], authors proposed two main discrete ESO.

The first one is Predictive Discrete Extended State Observer (PDESO), for which the following equations are applied:

$$\begin{aligned} z(k+1) &= \Phi z(k) + \Gamma u(k) + L_p[y(k) - z_1(k)]; \\ \overline{z}(k) &= z(k). \end{aligned} \tag{24}$$

The second one is Current Discrete Extended State Observer (CDESO), for which the following equations are applied:

$$\begin{aligned} z(k+1) &= \Phi z(k) + \Gamma u(k) + L_p[y(k) - z_1(k)]; \\ \overline{z}(k) &= z(k) + L_c[y(k) - z_1(k)]. \end{aligned} \tag{25}$$

The different matrices for Euler Discretization are

$$\begin{aligned} \Phi &= \begin{bmatrix} 1 & h & 0 \\ 0 & 1 & h \\ 0 & 0 & 1 \end{bmatrix}, \quad L_p = \begin{bmatrix} 3(1-\alpha) \\ 3\dfrac{(1-\alpha)^2}{h} \\ \dfrac{(1-\alpha)^3}{h^2} \end{bmatrix}, \\ \Gamma &= \begin{bmatrix} 0 \\ \hat{a}h \\ 0 \end{bmatrix}, \quad L_c = \begin{bmatrix} 1-\alpha^3 \\ \dfrac{(1-\alpha)^2(2+\alpha)}{h} \\ \dfrac{(1-\alpha)^3}{h^2} \end{bmatrix}. \end{aligned} \tag{26}$$

These matrices for ZOH Discretization are

$$\Phi = \begin{bmatrix} 1 & h & \dfrac{h^2}{2} \\ 0 & 1 & h \\ 0 & 0 & 1 \end{bmatrix}, \quad L_p = \begin{bmatrix} 3(1-\alpha) \\ 3\dfrac{(1-\alpha)^2(5+\alpha)}{2h} \\ \dfrac{(1-\alpha)^3}{h^2} \end{bmatrix}, \tag{27}$$

$$\Gamma = \begin{bmatrix} \hat{a}\dfrac{h^2}{2} \\ \hat{a}h \\ 0 \end{bmatrix}, \quad L_c = \begin{bmatrix} 1-\alpha^3 \\ 3\dfrac{(1-\alpha)^2(1+\alpha)}{2h} \\ (1-\alpha)^3/T^2 \end{bmatrix}. \tag{27}$$

Discretization of nonlinear ADRC. Authors in [11] proposed a discrete form of TD in order to avoid introducing considerable numerical errors in a discrete-time implementation. This discrete form is obtained as follows:

$$\begin{aligned} v_1 &= v_1 + hv_2; \\ v_2 &= v_2 + hv, \ \ |v| \le r, \end{aligned} \tag{28}$$

where v is written in the form

$$v = f_{han}(v_1 - v_0, v_2, r, h). \tag{29}$$

Here v_0 is the input signal, v_1 is the tracking signal of v_0, v_2 is the differential signal of v_1, r is the parameter which determines the tracking speed, is the sampling time and f_{han} is:

$$\begin{aligned} &d = hr^2; \quad a_0 = hv_2; \quad y_0 = v_1 + a_0; \\ &a_1 = \sqrt{d(d + 8|y|)}; \quad a_2 = a_0 + \operatorname{sign} y_0 \frac{(a_1 - d)}{2}; \\ &s_y = \frac{\operatorname{sign}(y_0 + d) - \operatorname{sign}(y_0 - d)}{2}; \\ &a_f = (a_0 + y_0 - a_2)s_y + a_2; \\ &s_a = \frac{\operatorname{sign}(a_f + d) - \operatorname{sign}(a_f - d)}{2}; \\ &f_{han} = -r\left(\frac{a_f}{d} - \operatorname{sign} a_f\right)s_a - r \operatorname{sign} a_f. \end{aligned} \tag{30}$$

Authors in [11] proposed a discrete implementation of the extended state observer ESO as follows:

$$\begin{aligned} &e = z_1 - y; \\ &fe = f_{\mathrm{ESO}}(e, 0.5, \eta); \qquad fe_1 = f_{\mathrm{ESO}}(e, 0.25, \eta); \\ &z_1 = z_1 + hz_2 + \alpha_1 e; \\ &z_2 = z_2 + h(z_3 + \hat{a}u) + \alpha_2 fe; \\ &z_3 = z_3 + \alpha_3 fe_1; \\ &f_{\mathrm{ESO}}(e, \zeta, \eta) = \begin{cases} |e|^{\zeta} \operatorname{sign} e, & |e| > \eta, \\ e/\left(\eta^{1-\zeta}\right), & |e| \le \eta, \end{cases} \qquad \eta > 0, \end{aligned} \tag{31}$$

where h is the sampling time and ζ is the nonlinearity factor.

Finally, control and rejection scheme parts are the same as for the continuous implementation, i.e.,

$$\begin{aligned} \hat{e}_1 &= v_1 - z_1; \\ \hat{e}_2 &= v_2 - z_2; \\ u_0 &= \beta_1 f_{\text{ESO}}(\hat{e}_1, \gamma_1, \eta) + \beta_2 f_{\text{ESO}}(\hat{e}_2, \gamma_2, \eta); \\ u &= u_0 - \frac{z_3}{a}. \end{aligned} \tag{32}$$

Discrete nonlinear ADRC parameters selection. There are two parameters in TD, $[r, h]$, six in ESO, $[\alpha_1, \alpha_2, \alpha_3, \zeta_1, \zeta_2, a]$ and five in NLSEF, $[\beta_1, \beta_2, \gamma_1, \gamma_2, \eta]$. In general there are 13 parameters, these parameters are determined empirically. ADRC suffers from very limited application due to its complicated parameters adjustment. To overcome this problem, key parameters of ADRC are usually adjusted in two stages. In the first stage, parameters are roughly adjusted to estimate the ballpark ranges. In the second stage, further optimization of the parameters with specific algorithm is done to determine the precise adjustment. Genetic Algorithm (GA), and Particle Swarm Optimization (PSO) have been widely used in the optimization process to determine optimal ADRC parameters. In order to facilitate estimation of the parameters, they can be divided into key parameters and common parameters [8]. Key parameters are $[\alpha_1, \alpha_2, \alpha_3, \beta_1, \beta_2]$, on which optimization process is applied.

Case Study: ADRC for quarter-car active suspension system. Comfort is a very important issue for passengers when they travel from one place to another. During traveling, a car may encounter various vibrations and shocks from ground. These vibrations may cause problems to passengers. To overcome these problems, loads from ground should be damped out. Automotive suspension systems are intended to absorb and decrease the shocks and vibrations transferred from the ground to the passengers as well as to the vehicle body. Traditionally, passive suspension system is used to absorb vibrations in many different types of vehicles. Active suspension systems separate actuators to apply controlled forces and provide better ride.

The suspension system shown in Fig. 3 represents vehicle system at each wheel. It consists of a spring k_s, a damper b_s and a hydraulic actuator F_a. In addition, k_t represents tire stiffness and b_t represents tire damping. The effective vehicle body mass is expressed by M_s (sprung mass), and M_u (unsprung mass) represents the effective mass for the wheel and the axle. States x_u, x_s represent the vertical displacements from the static equilibrium for M_u

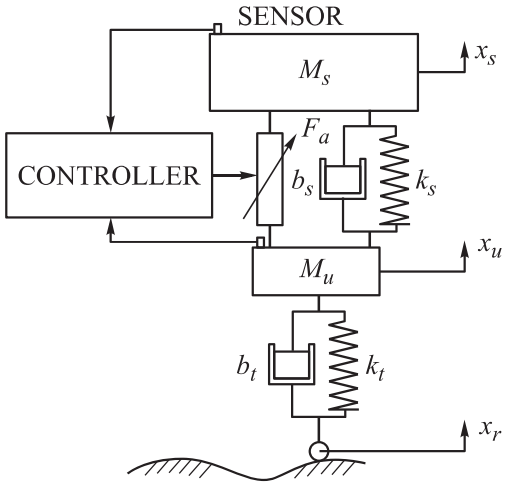

Fig. 3. Quarter-car active suspension system

and M_s respectively. The road profile is represented by x_r. The suspension travel $x_s - x_u$ is measured and compared to the set point $(v_0 = 0)$.

The required actuator force is determined by the controller to eliminate errors, and thus, to reduce the vehicle oscillations. The actuator can provide a maximum force of 3 000 N.

Table 1 shows the approximated values of the system parameters.

Table 1

Approximated values of the quarter-car system parameters

Parameter	Unit	Value	Parameter	Unit	Value
M_s	kg	300	k_t	N / m	180 000
M_u	kg	50	b_s	N·s / m	1 200
k_s	N / m	18 000	b_t	N·s / m	0

Vibration model of the sprung and unsprung masses can be expressed by the following dynamic equations:

$$\begin{aligned} M_u\ddot{x}_u &= k_s(x_s - x_u) + b_s(\dot{x}_s - \dot{x}_u) - k_t(x_u - x_r) - b_t(\dot{x}_u - \dot{x}_r) - F_a; \\ M_s\ddot{x}_s &= -k_s(x_s - x_u) - b_s(\dot{x}_s - \dot{x}_u) + F_a. \end{aligned} \tag{33}$$

However, Mohite, et al. in [13] proposed a nonlinear model for the passive quarter-car system. In their work, tire stiffness k_t for the linear system can vary as k_{t1}, k_{t2}, k_{t3} for considering of nonlinearity. In the same manner, k_s can vary as k_{s1}, k_{s2}, and b_s as b_{s1}, b_{s2}. In this way, equations of motion can be expressed in the following nonlinear form:

$$\begin{aligned} M_u\ddot{x}_u = {} & k_{s1}(x_s - x_u) + k_{s2}(x_s - x_u)^3 + b_{s1}(\dot{x}_s - \dot{x}_u) + b_{s2}(\dot{x}_s - \dot{x}_u)^2 - \\ & - k_{t1}(x_u - x_r) - k_{t2}(x_u - x_r)^2 + k_{t3}(x_u - x_r)^3 - b_t(\dot{x}_u - \dot{x}_r) - F_a; \\ M_s\ddot{x}_s = {} & -k_{s1}(x_s - x_u) - k_{s2}(x_s - x_u)^3 - b_{s1}(\dot{x}_s - \dot{x}_u) - b_{s2}(\dot{x}_s - \dot{x}_u)^2 + F_a. \end{aligned} \quad (34)$$

Table 2 shows the approximated values of the nonlinear system parameters.

Table 2

Approximated values of the quarter-car nonlinear system parameters

Parameter	Unit	Value	Parameter	Unit	Value
M_s	kg	295	k_{t2}	N / m	42 509
M_u	kg	39	k_{t3}	N / m	22 875
k_{s1}	N / m	15 302	b_{s1}	N·s / m	3 482
k_{s2}	N / m	2 728	b_{s2}	N·s / m	580
k_{t1}	N / m	60 063	b_t	N·s / m	0

Control of quarter-car model using linear ADRC. Simulink blocks have been built to represent linear and nonlinear models for simulating control of quarter-car active suspension system. LTD, PD and LESO blocks have been built as in the first section. Closed loop pole w_{CL} is usually chosen empirically as a trade-off between states approximation convergence speed and the influence of both sampling time and noise [14]. However; $w_{CL} = 1.7$ is found to be a good choice. The estimated value of a from equation (2) is chosen empirically to be $\hat{a} = 0.001$.

Linear ADRC is simulated for studying the control of the linear and nonlinear models of quarter-car system. Moreover; using this simulation, a comparison is made between this system performance and the performance of the passive system. Passive suspension system is simulated by applying a constant input $F_a = 0$ when the controller is not activated. Two types of road disturbance are tested: a double bump disturbance and random disturbance. The double bump is described by equation, where w is the sudden bump, h_b is the bump

height, t_0 is the bump initiating time, x_t is a time delay, V is the car speed, μ is an arbitrary constant and λ is the disturbance wavelength

$$w(t) = \begin{cases} 0.5h_b\left(1 - \cos\left(\dfrac{2\pi V(t - t_0)}{\lambda}\right)\right), & t_0 \le t \le t_0 + \dfrac{\lambda}{V}; \\ 0.5\mu h_b\left(1 - \cos\left(\dfrac{2\pi V(t - t_0 - x_t)}{\lambda}\right)\right), & t_0 + x_t \le t_f \le t_0 + x_t + \dfrac{\lambda}{V}; \\ 0 \quad \text{otherwise.} \end{cases} \quad (35)$$

Fig. 4 shows the bump signal that corresponds to the following parameters $V = 45$ km/h; $h_b = 0.1$ m; $t_0 = 4$ s; $\mu = 1$ m and $x_t = 1$ s.

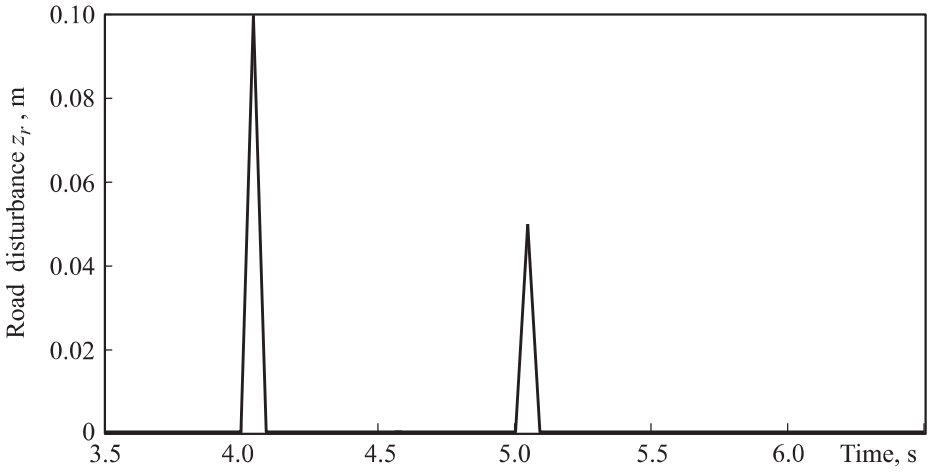

Fig. 4. Double bump road disturbance

Random road disturbance is randomly filtered as in [15] which has clear physical meaning and easy computing character:

$$\dot{q}(t) = -2\pi f_0 q(t) + 2\pi n_0 \sqrt{G_q(n_0)v}\, w(t), \quad (36)$$

where f_0 is the filter lower-cut-off frequency, $q(t)$ is the random road input signal, $G_q(n_0)$ is the road roughness coefficient and $w(t)$ is a Gaussian white noise. The following parameters are considered: an integration filter ($f_0 = 0$), the vehicle speed is $v = 20$ m/s driving is on a class D road for which $G_q(n_0) = 1\,024 \cdot 10^{-6}$ (see [15]).

Fig. 5 shows both responses of passive and linear ADRC control systems to a double bump road disturbance which was shown in Fig. 4. It is obvious that linear ADRC compensates for disturbances and leads the system to enter the stability region faster.

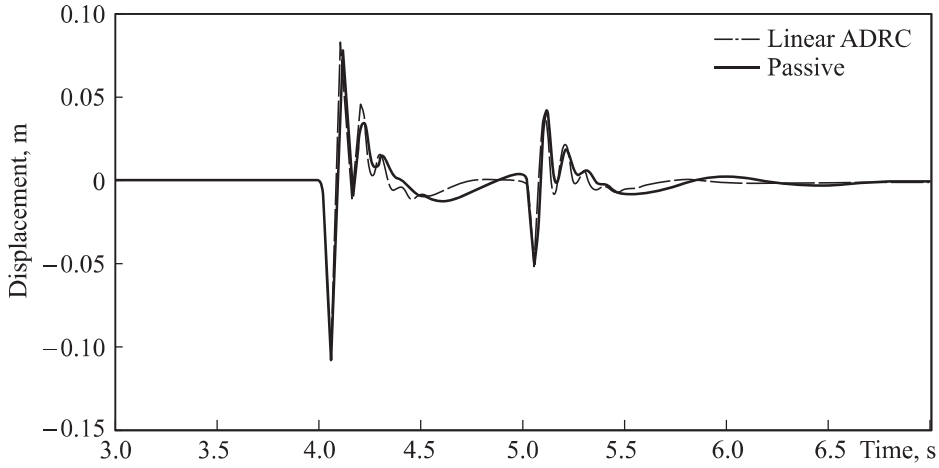

Fig. 5. ADRC and Passive control systems responses for double bump disturbance

Fig. 6 shows the estimated values for the output y during the process. Fig. 7 shows the estimated values for the output rate $\dot{y}$. It is clear that there is a good estimation for the displacement but a poor one for its rate. To improve rate estimation, the output acceleration could be taken as a second output. However, it's not the subject of this research.

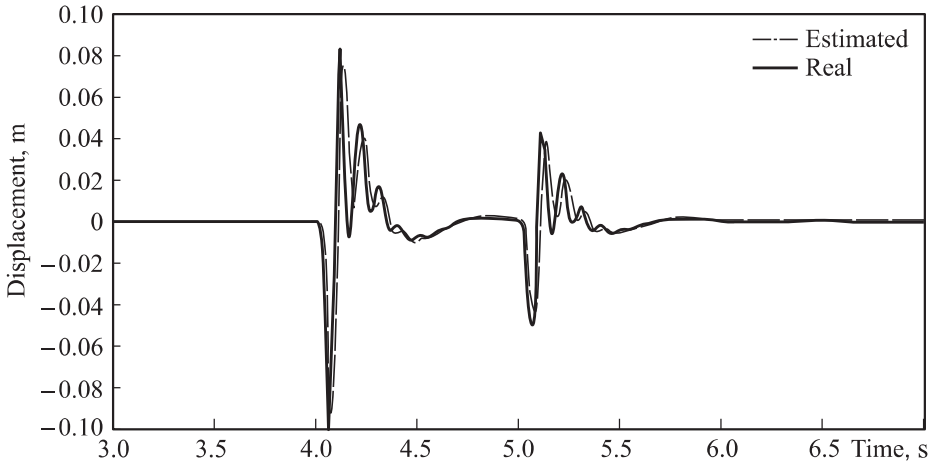

Fig. 6. Linear ADRC ESO estimation for the output signal

Fig. 8 shows both responses of passive and linear ADRC control systems to the random road disturbance described in equation (36). The ability of linear ADRC to compensate for disturbances is clear. To verify the control efficiency for random disturbance, root mean square (RMS) values are calculated for the passive and the controlled system. Using MATLAB, the following values are found for RMS:

RMS for Passive system output is 0.0118;
RMS for linear ADRC controlled system output is 0.009.
This means that the disturbance density is reduced by 25 %.

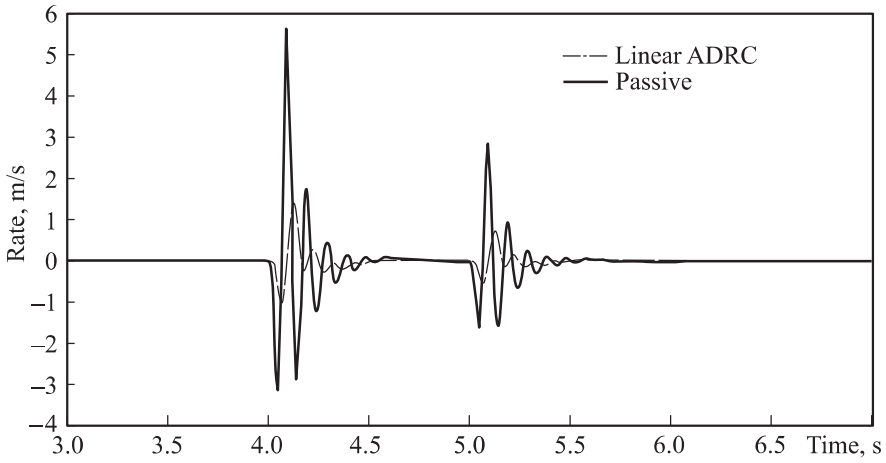

Fig. 7. Linear ADRC ESO estimation for the output signal rate

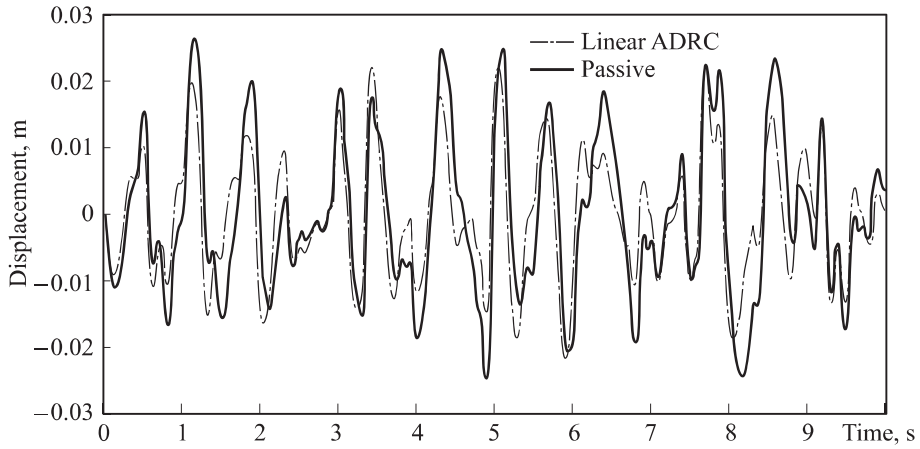

Fig. 8. Linear ADRC for random road disturbance

Now the ability of linear ADRC to compensate for dynamic uncertainties could be tested by simulating it for the nonlinear quarter-car system.

Here, the nonlinear equations (34) are simulated in the presence of an actuator model in the form of equation (37), where $\tau = 70$ s is the actuator's pole and $T = 0.015$ s is the actuator's delay.

$$y_{act} = \begin{cases} \dfrac{e^{-T}}{1+\tau}u, & -1\,500 \le u \le 1\,500; \\ -1\,500, & u < -1\,500; \\ 1\,500, & u > 1\,500. \end{cases} \qquad (37)$$

It can be seen from Fig. 9 that linear ADRC controller slightly compensates for the different nonlinearities of the system. This compensation could be made better by retuning the ADRC parameters or moving to a nonlinear ADRC.

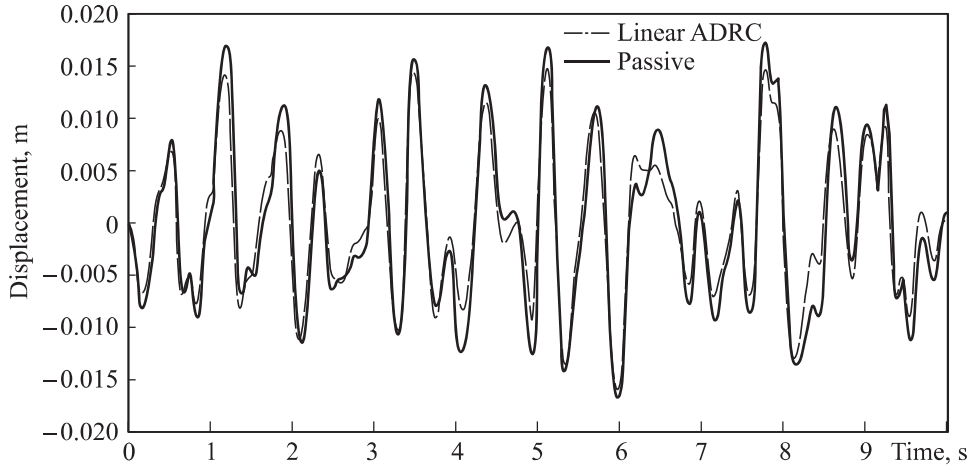

Fig. 9. Linear ADRC vs passive system performance for nonlinear quarter-car system

Control of quarter-car model using nonlinear ADRC. In this section the discrete version of the nonlinear ADRC is used. Parameters are chosen as in Table 3.

Table 3

Tuning parameters for nonlinear ADRC

Key parameters		General parameters	
α_1	$3w_{\text{ESO}}$	r	20
α_2	$3w_{\text{ESO}}^2$	h	0.01
α_3	w_{ESO}^3	γ_1	0.4
β_1	1	γ_2	0.6
β_2	50	ζ_1	0.5
–	–	ζ_2	0.25
–	–	η	1.5

In Table 3 α_1, α_2, α_3 are chosen similarly as in the linear ADRC.

Fig. 10 shows responses of both the passive and the nonlinear ADRC control systems to the double bump road disturbance shown in Fig. 4. In this figure, the ability of nonlinear ADRC to compensate for disturbances and damp them faster is clear.

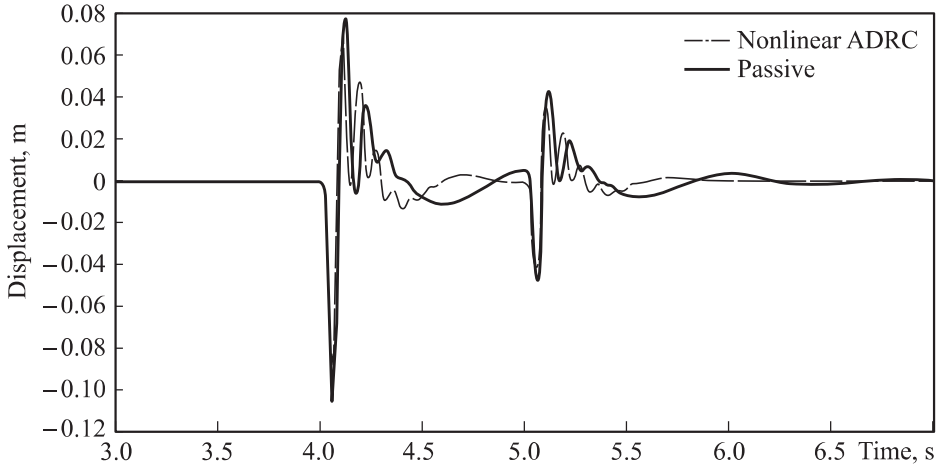

Fig. 10. Double bump response of quarter-car system controlled by nonlinear ADRC

Fig. 11 shows responses of both the passive and the nonlinear ADRC control systems to the random road disturbance described in equation (36). RMS values for passive and nonlinear ADRC systems outputs are:

RMS (for Passive system output) is 0.0118;

RMS (for nonlinear ADRC controlled system output) is 0.008.

This means that disturbance density is reduced by 33 %.

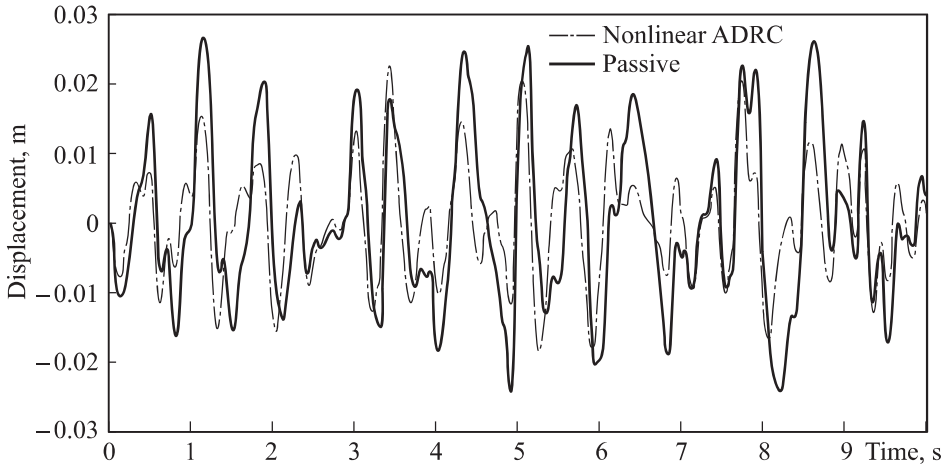

Fig. 11. Random road disturbance response of quarter-car system controlled by nonlinear ADRC

It can be noticed that the output RMS value here is a little better than the RMS value for linear ADRC. This is due to the nonlinear functions used in ESO.

Again, the ability of the nonlinear ADRC to compensate for dynamic uncertainties could be tested by simulation in the nonlinear quarter-car system.

Fig. 12 shows that nonlinear ADRC controller compensates for the different nonlinearities of the system. RMS values for passive and nonlinear ADRC systems outputs are:

RMS (for Passive system output) is 0.0081;

RMS (for nonlinear ADRC controlled system output) is 0.006.

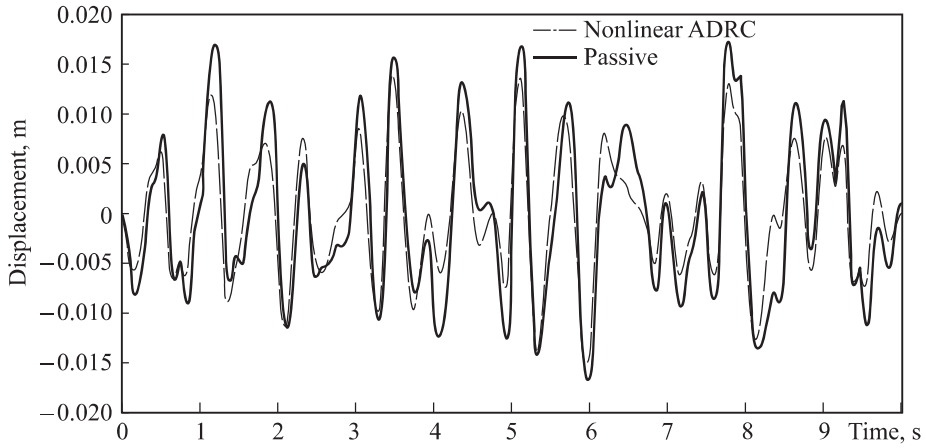

Fig. 12. Nonlinear ADRC vs passive system performance for nonlinear quarter-car system

This means that the disturbance density is reduced by 30 % and the nonlinear ADRC shows better performance than the linear one.

Conclusion. In this work, two main approaches of the second order ADRC are presented: linear and nonlinear ADRC. Both approaches consist of two loops: feedback loop and estimation loop. The three main components: controller, estimator and disturbance rejection scheme for each approach are presented. Tuning and selection parameters for both approaches are discussed. Discrete implementation forms for both approaches are presented. A simple linear and nonlinear quarter-car models are used as a study case. Active suspension system controlled by ADRC is tested against passive system. Simulation results show a good ADRC performance and efficiency against internal and external disturbances.

Translated by Authors

REFERENCES

[1] Qing Z., Gao Z. On practical applications of active disturbance rejection control. *Proc. 29th Chinese Control Conf.*, 2010.
Available at: https://ieeexplore.ieee.org/document/5572922

[2] Qian L., Li D., Tan W. Design of multi-loop ADRC controllers based on the effective open-loop transfer function method. *Proc. 33rd Chinese Control Conf.*, 2014. DOI: https://doi.org/10.1109/ChiCC.2014.6895546

[3] Xue W., Bai W., Yang S., et al. ADRC with adaptive extended state observer and its application to air–fuel ratio control in gasoline engines. *IEEE Trans. Ind. Electron.*, 2015, vol. 62, no. 9, pp. 5847–5857. DOI: https://doi.org/10.1109/TIE.2015.2435004

[4] Li F., Zhang Z., Armaou A., et al. Study on ADRC parameter optimization using CPSO for clamping force control system. *Math. Probl. Eng.*, 2018, vol. 2018, art. 2159274. DOI: https://doi.org/10.1155/2018/2159274

[5] Zhu E., Pang J., Sun N., et al. Airship horizontal trajectory tracking control based on active disturbance rejection control (ADRC). *Nonlinear Dynamics*, 2014, vol. 75, pp. 725–734.

[6] Li X., Wang S., Wang X., et al. Permanent magnet brushless motor control based on ADRC. *MATEC Web Conf.*, 2016, vol. 40, art. 08003. DOI: https://doi.org/10.1051/matecconf/20164008003

[7] Gao Z., Tian G. Extended active disturbance rejection controller. Patent US 8180464. Appl. 20.08.2008, publ. 01.01.2009.

[8] Peng C., Tian Y., Bai Y., et al. ADRC trajectory tracking control based on PSO algorithm for a quad-rotor. *ICIEA*, 2013, pp. 800–805. DOI: https://doi.org/10.1109/ICIEA.2013.6566476

[9] Han J.Q. From PID technique to active disturbance rejection control technique. *Control Engineering of China*, 2002, vol. 9, no. 3, pp. 13–18.

[10] Wang Ch., Zhang H., Yu Y. USV trajectory tracking control system based on ADRC. *CAC*, 2017, pp. 7534–7538. DOI: https://doi.org/10.1109/CAC.2017.8244141

[11] Han J. From PID to active disturbance rejection control. *IEEE Trans. Ind. Electron.*, 2009, vol. 56, no. 3, pp. 900–906. DOI: https://doi.org/10.1109/TIE.2008.2011621

[12] Zhou X., Yang C., Zhao B., et al. A high-precision control scheme based on active disturbance rejection control for a three-axis inertially stabilized platform for aerial remote sensing applications. *J. Sens.*, 2018, vol. 2018, art. 7295852. DOI: https://doi.org/10.1155/2018/7295852

[13] Mohite A.G., Mitra A.C. Development of linear and non-linear vehicle suspension model. *Mater. Today*, 2018, vol. 5, no. 2-1, pp. 4317–4326. DOI: https://doi.org/10.1016/j.matpr.2017.11.697

[14] Madoński R., Herman P. An experimental verification of ADRC robustness on a cross-coupled aerodynamical system. *IEEE Int. Symp. Industrial Electronics*, 2018, pp. 859–863. DOI: https://doi.org/10.1109/ISIE.2011.5984271

[15] Zhou Q. Research and simulation on new active suspension control system. Master Thesis. Lehigh University, 2013.

Alhelou M. — Post-Graduate Student, Department of Automatic Control Systems, Bauman Moscow State Technical University (2-ya Baumanskaya ul. 5, str. 1, Moscow, 105005 Russian Federation).

Gavrilov A.I. — Cand. Sc. (Eng.), Assoc. Professor, Department of Automatic Control Systems, Bauman Moscow State Technical University (2-ya Baumanskaya ul. 5, str. 1, Moscow, 105005 Russian Federation).

Please cite this article as:

Alhelou M., Gavrilov A.I. Synthesis of active disturbance rejection control. *Herald of the Bauman Moscow State Technical University, Series Instrument Engineering*, 2020, no. 4, pp. 22–41. DOI: https://doi.org/10.18698/0236-3933-2020-4-22-41